LETTER • OPEN ACCESS

Vacuum solution for Solov'ev's equilibrium configuration in tokamaks

To cite this article: Tao Xu and Richard Fitzpatrick 2019 *Nucl. Fusion* **59** 064002

OPEN ACCESS
IOP Publishing | International Atomic Energy Agency
Nuclear Fusion
Nucl. Fusion **59** (2019) 064002 (8pp)
https://doi.org/10.1088/1741-4326/ab1ce3

Letter

Vacuum solution for Solov'ev's equilibrium configuration in tokamaks

Tao Xu[1,2] **and Richard Fitzpatrick**[1]

[1] Department of Physics, Institute for Fusion Studies, University of Texas at Austin, Austin, TX 78712, United States of America
[2] Institute of Fusion and Plasma Research, College of Electrical and Electronic Engineering, Huazhong University of Science and Technology, Wuhan 430074, China

E-mail: xutao@hust.edu.cn

Received 28 February 2019, revised 5 April 2019
Accepted for publication 26 April 2019
Published 13 May 2019

Abstract

In this work, we construct a tokamak plasma equilibrium generated by a combination of currents flowing within the plasma and in distant external magnetic field coils. The plasma toroidal current density takes the simple form $j_\varphi(r,z) = -a\,r - b\,R^2/r$ inside the plasma (where r and z are cylindrical coordinates, and a, b, and R are constants), and is zero in the surrounding vacuum. The Grad–Shafranov equation possesses a well-known exact analytic solution within the plasma due to Solov'ev. We use a Green's function method to compute the poloidal magnetic flux generated by plasma currents, together with a parameterized homogeneous solution to the Grad–Shafranov equation (that is well-behaved at small r and z), to construct the vacuum solution. The vacuum solution is matched to the analytic solution on the last closed magnetic flux surface (LCFS) to determine the parameters in the homogeneous solution. This procedure is performed for both up–down-symmetric double-null and up–down-asymmetric single-null equilibria. We find that any magnetic X-points on the LCFS are distorted due to the fact that one quadrant is filled by a current-carrying plasma, whereas the other three are filled by a vacuum in which no current flows. In particular, the vacuum quadrant opposite the plasma-filled quadrant expands at the expense of the other three quadrants.

Keywords: plasma equilibrium, Grad–Shafranov equation, homogeneous solution

1. Introduction

Calculation of plasma equilibria is a crucial component in the design and operation of the magnetic confinement devices employed in nuclear fusion research. The equilibrium poloidal flux in axisymmetric toroidal magnetic confinement devices is determined by solving the Grad–Shafranov equation [1–3], which is a nonlinear, elliptic, partial differential equation. The solution of the Grad–Shafranov equation is usually effected via an iterative numerical scheme.

In 1968, Solov'ev [4] obtained a family of exact analytic solutions of the Grad–Shafranov equation. Solov'ev's solutions are useful for benchmarking plasma equilibrium codes [5, 6], as well as for magnetohydrodynamical stability analysis of tokamak plasmas [7]. Solov'ev's solutions have been employed to construct model up–down-symmetric tokamak equilibria [8], as well as equilibria with magnetic divertors. Recently, more advanced analytic solutions of the Grad–Shafranov equation have been obtained that allow for a wide variety of different plasma configurations [9–11].

Solov'ev's analytic solutions of the Grad–Shafranov equation (as well as the other aforementioned analytic solutions) are derived on the assumption that there is distributed toroidal current filling all space. In reality, the plasma current density is zero in the vacuum region that lies beyond the last closed (magnetic) flux surface (LCFS). Now, the solution of the Grad–Shafranov equation in the vacuum region consists of two components. The first component is the contribution from the toroidal currents flowing within the plasma. The second component is the contribution from currents flowing in external magnetic field coils. In this study, for the sake of simplicity, the external field coils are assumed to be very distant from the plasma. In order to construct the correct solution in the vacuum region, we use a Green's function method to compute the contribution from the plasma currents, and then combine this with a parameterized homogeneous solution of the Grad–Shafranov equation that is well behaved on the toroidal symmetry axis. The parameters that characterize the homogeneous solution are determined by demanding that, when the homogeneous solution is added to the plasma solution, the net solution is constant on the LCFS. In this manner, we obtain a realistic vacuum solution that is consistent with Solov'ev's analytic solution within the plasma.

This paper is organized as follows. The Grad–Shafranov equation is introduced in section 2. Solov'ev's analytic solution, and its problem, is discussed in section 3. Our method for obtaining the vacuum field for up–down-symmetric double-null equilibria is presented in section 4. Our method is extended to deal with up–down-asymmetric single-null equilibria in section 5. The paper is summarized in section 6.

2. Grad–Shafranov equation

Let r, φ, z be conventional cylindrical coordinates. In the following, all lengths are normalized to some convenient scale length, R_0, all magnetic field strengths to some convenient scale field, B_0, all poloidal magnetic fluxes to $R_0^2\,B_0$, all toroidal current densities to $B_0/(\mu_0\,R_0)$, and all plasma pressures to B_0^2/μ_0. (In fact, B_0 is the vacuum toroidal magnetic field strength at $r = R_0$.) Consider an axisymmetric toroidal plasma equilibrium whose magnetic field is written

$$\mathbf{B} = \frac{I_A}{r}\,\mathbf{e}_\varphi + \frac{\nabla\psi\times\mathbf{e}_\varphi}{r}. \tag{1}$$

Here, $\psi(r,z)$ is the poloidal magnetic flux, and $I_A(\psi)$ is an arbitrary flux function that takes the value unity in the vacuum region surrounding the plasma. As is well known, the poloidal flux satisfies the Grad–Shafranov equation [1–3],

$$\frac{\partial^2\psi}{\partial z^2} + r\,\frac{\partial}{\partial r}\left(\frac{1}{r}\,\frac{\partial\psi}{\partial r}\right) = -r\,j_\varphi, \tag{2}$$

where

$$j_\varphi(r,z) = r\,p' + \frac{I_A\,I_A'}{r} \tag{3}$$

is the toroidal current density. Here $p(\psi)$ is the plasma pressure, which is an arbitrary flux function that takes the value zero in the vacuum region surrounding the plasma. Moreover, $'$ denotes a derivative with respect to argument.

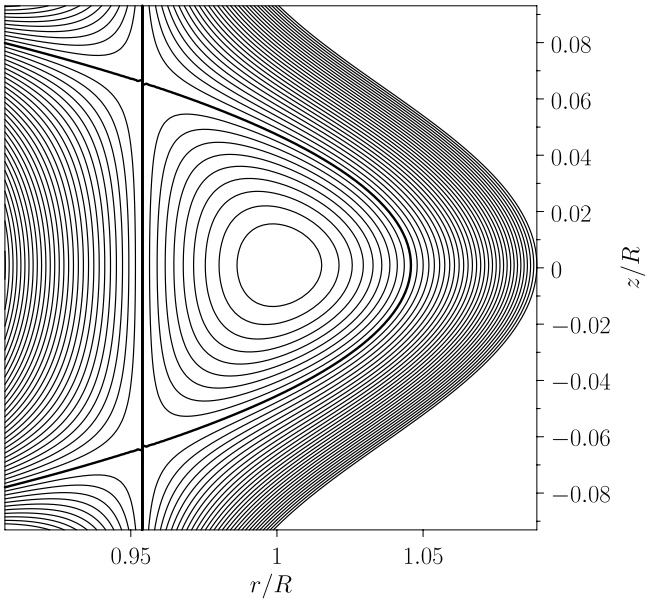

Figure 1. Contours of $\psi(r,z)$ calculated by Solov'ev's method for a double-null magnetic equilibrium with $R = 1.0$, $a = 1.2$, $b = -1.0$, and $c_0 = 1.1$.

3. Solov'ev's solution and its problem

Following Solov'ev [4], let us assume that

$$p' = -a, \tag{4}$$

$$I_A\,I_A' = -b\,R^2, \tag{5}$$

where a, b, and R are constants. This implies that

$$j_\varphi(r,z) = -a\,r - \frac{b\,R^2}{r}. \tag{6}$$

In this case, equation (2) possesses the exact analytic solution [4]

$$\psi(r,z) = \frac{1}{2}\,(b+c_0)\,R^2\,z^2 + c_0\,R\,\zeta\,z^2 + \frac{1}{2}\,(a-c_0)\,R^2\,\zeta^2, \tag{7}$$

where c_0 is a constant, and

$$\zeta = \frac{r^2 - R^2}{2\,R}. \tag{8}$$

As illustrated in figure 1, for $a > c_0 > -b$, the contours of $\psi(r,z)$ map out a family of up–down-symmetric plasma equilibria with positive triangularity. The magnetic axis is located at $r = R$, $z = 0$. Note that $\psi = 0$ on the axis. The magnetic flux surfaces in the immediate vicinity of the magnetic axis are nested ellipses whose major radii are aligned with the r and z axes. The constant ratio of the major radii of these ellipses is $l_z/l_r = [(a-c_0)/(b+c_0)]^{1/2}$. The magnetic configuration possesses two magnetic X-points, located at $\zeta = \zeta_X$ and $z = \pm z_X$, where

$$\zeta_X = -\left(\frac{b+c_0}{2\,c_0}\right) R, \tag{9}$$

$$z_X = \left[\frac{(b+c_0)\,(a-c_0)}{2\,c_0^2}\right]^{1/2} R. \tag{10}$$

Both X-points lie on the LCFS, $\psi = \psi_X$, where

$$\psi_X = \frac{(a-c_0)\,(b+c_0)^{\,2}\,R^4}{8\,c_0^2} > 0. \tag{11}$$

Generally speaking, we expect the region beyond the LCFS to be a vacuum (or near vacuum) in which the plasma current density is zero. However, according to equation (6), Solov'ev's analytic solution of the Grad–Shafranov equation assumes a toroidal current density distribution that extends to infinity, and is, therefore, not zero in the vacuum region. It is precisely this deficiency of the Solvov'ev solution that we aim to remedy in our paper.

4. Our method for double-null equilibria

Suppose that the toroidal current density within the plasma is the same as that assumed in the Solov'ev calculation, but that there is zero current density in the vacuum region outside the LCFS. Now, the poloidal magnetic flux in the vacuum region consists of two components. The first component, $\psi_p(r,z)$, is the flux generated by the known toroidal current distribution within the LCFS. We will use a Green's function method to compute this component. The second component, $\psi_h(r,z)$, is the contribution from currents flowing in remote external magnetic field coils. This component is a homogeneous solution to the Grad–Shafranov equation that is well behaved at small r and z.

In order to calculate $\psi_p(r,z)$, it is helpful to define the flux coordinates ψ and θ, where

$$\tan\theta = \frac{z}{\zeta}. \tag{12}$$

At given values of ψ and θ, we can determine ζ by combining equations (7) and (12) to give the cubic equation

$$(c_0\,R\,\tan^2\theta)\,\zeta^3 + \left[\frac{1}{2}\,(b+c_0)\,\tan^2\theta\,R^2 + \frac{1}{2}\,(a-c_0)\,R^2\right]\zeta^2 - \psi = 0. \tag{13}$$

For $0 < \psi < \psi_X$ (i.e. within the LCFS), this equation possesses three real roots. For $\cos\theta > 0$ the largest root is appropriate, whereas the intermediate root is appropriate when $\cos\theta < 0$. Once ζ has been determined, z follows from equation (12).

Now,

$$\frac{\partial(\psi,\theta)}{\partial(\zeta,z)} = \begin{vmatrix} \partial\psi/\partial\zeta, & \partial\psi/\partial z \\ \partial\theta/\partial\zeta, & \partial\theta/\partial z \end{vmatrix}, \tag{14}$$

where

$$\frac{\partial\psi}{\partial\zeta} = c_0\,R\,z^2 + (a-c_0)\,R^2\,\zeta, \tag{15}$$

$$\frac{\partial\psi}{\partial z} = (b+c_0)\,R^2\,z + 2\,c_0\,R\,\zeta\,z, \tag{16}$$

$$\frac{\partial\theta}{\partial\zeta} = -\frac{z}{\zeta^2+z^2}, \tag{17}$$

$$\frac{\partial\theta}{\partial z} = \frac{\zeta}{\zeta^2+z^2}, \tag{18}$$

which implies that

$$\frac{\partial(\psi,\theta)}{\partial(\zeta,z)} = \frac{3\,c_0\,R\,\zeta\,z^2 + (a-c_0)\,R^2\,\zeta^2 + (b+c_0)\,R^2\,z^2}{\zeta^2+z^2}. \tag{19}$$

Furthermore,

$$\frac{\partial(\zeta,z)}{\partial(r,z)} = \begin{vmatrix} \partial\zeta/\partial r, & \partial\zeta/\partial z \\ \partial z/\partial r, & \partial z/\partial z \end{vmatrix} = \frac{\partial\zeta}{\partial r} = \frac{r}{R}, \tag{20}$$

which yields

$$\frac{\partial(\psi,\theta)}{\partial(r,z)} = \frac{\partial(\psi,\theta)}{\partial(\zeta,z)}\,\frac{\partial(\zeta,z)}{\partial(r,z)} = r\left[\frac{3\,c_0\,\zeta\,z^2 + (a-c_0)\,R\,\zeta^2 + (b+c_0)\,R\,z^2}{\zeta^2+z^2}\right]. \tag{21}$$

The poloidal magnetic flux, $\psi_p(r,z)$, generated by the toroidal currents flowing within the plasma is written

$$\psi_p(r,z) = \int\int G(r,z;r',z')\,j_\varphi(r',z')\,\mathrm{d}r'\,\mathrm{d}z', \tag{22}$$

where the integral is over the plasma poloidal cross-section, and $j_\varphi(r,z)$ is given by equation (6). The Green's function takes the form [12]

$$G(r,z;r',z') = \frac{\sqrt{r\,r'}}{2\pi}\,\frac{[(2-k^2)\,K(k) - 2\,E(k)]}{k}, \tag{23}$$

where

$$k = \frac{\sqrt{4\,r\,r'}}{[(r+r')^{\,2} + (z-z')^{\,2} + \epsilon]^{\,1/2}}, \tag{24}$$

and

$$K(k) = \int_0^{\pi/2} \frac{\mathrm{d}\theta}{(1-k^2\,\sin^2\theta)^{\,1/2}}, \tag{25}$$

$$E(k) = \int_0^{\pi/2} (1-k^2\,\sin^2\theta)^{\,1/2}\,\mathrm{d}\theta. \tag{26}$$

It follows that

$$\psi_p(r,z) = -\int_0^{(1-\eta)\,\psi_X} \oint \frac{\sqrt{r\,r'}}{2\pi}\,\frac{[(2-k^2)\,K(k)-2\,E(k)]}{k}\left(a\,r'+\frac{b\,R^2}{r'}\right) \times\left[\frac{\partial(\psi,\theta)}{\partial(r',z')}\right]^{-1} \mathrm{d}\psi\,\mathrm{d}\theta, \tag{27}$$

or

$$\psi_p(r,z) = -\int_0^{(1-\eta)\,\psi_X} \oint \frac{\sqrt{r\,r'}}{2\pi}\,\frac{[(2-k^2)\,K(k)-2\,E(k)]}{k}\left(a+\frac{b\,R^2}{r'^2}\right) \times\left[\frac{\zeta'^2+z'^2}{3\,c_0\,\zeta'\,z'^2+(a-c_0)\,R\,\zeta'^2+(b+c_0)\,R\,z'^2}\right] \mathrm{d}\psi\,\mathrm{d}\theta, \tag{28}$$

where

$$0 = \left(c_0\,R\,\tan^2\theta\right)\zeta'^3+\left[\frac{1}{2}\,(b+c_0)\,\tan^2\theta\,R^2+(a-c_0)\,R^2\right]\zeta'^2-\psi, \tag{29}$$

$$r' = \sqrt{2\,R\,\zeta'+R^2}, \tag{30}$$

$$z' = \tan\theta\;\zeta'. \tag{31}$$

Here, ϵ and η are small regularization parameters.

The poloidal magnetic flux, $\psi_h(r,z)$, generated by currents flowing in distant magnetic field coils is written [13]

$$\psi_h(r,z) = \sum_{N=0,N_h-1} c_N\,\psi_{2N}(r,z), \tag{32}$$

where the c_N are arbitrary coefficients,

$$\psi_N(r,z) = \sum_{n=0,N/2-1} A_N^n\,r^{N-2\,n}\,z^{2\,n}, \tag{33}$$

and

$$A_N^n = -\frac{(N/2+1-n)\,(N/2-n)}{n\,(n-1/2)}\,A_N^{n-1} \tag{34}$$

for $1 \leqslant n \leqslant N/2-1$, with $A_N^0 = 1$. Note that the sum (32) is truncated at $N = N_h - 1$.

The coefficients, c_N, that characterize the homogenous solution, (32), are determined by demanding that

$$\psi_p(r,z)+\psi_h(r,z) = (1-\eta)\,\psi_X \tag{35}$$

on the control surface $\psi = (1-\eta)\,\psi_X$. Given that there are N_h independent c_N values, the matching must be performed at N_h different values of θ. These values are evenly distributed in the range 0 to π, with a small common offset that is chosen so as to ensure that one of the matching points corresponds to the upper X-point on the LCFS. Note that, because of the up–down symmetry of the problem, any matching point in the upper half-plane ($z > 0$) is automatically accompanied by an equivalent matching point in the lower half-plane ($z < 0$). In other words, there are effectively $2\,N_h$ matching points on the LCFS.

Our first example is an up–down-symmetric double-null plasma equilibrium calculated with the following parameters: $R = 1.0$, $a = 1.2$, $b = -1.0$, and $c_0 = 1.1$. The corresponding Solov'ev solution is shown in figure 1.

In order to realize our method, the $\psi-\theta$ integral in expression (28) is implemented using a two-dimensional (2D) trapezium rule on a 1000×1000 uniform rectangular grid. The regularization parameters ϵ and η take the values 10^{-12} and 10^{-6}, respectively. We find that $\lambda \equiv |\psi(R,0)|/\psi_X$ is a good measure of the accuracy of both the integration scheme and the matching procedure. Of course, λ, which is the relative magnitude of the normalized poloidal magnetic flux on the magnetic axis, should be equal to zero. Obviously, if N_h is too small then the matching procedure is inaccurate because the truncated series (32) cannot adequately represent the true homogeneous solution of the Grad–Shafranov equation. On the other hand, if N_h is too large then the matching procedure becomes inaccurate due to rounding errors. We find that λ is minimized, taking the value 5×10^{-6}, when $N_h = 10$.

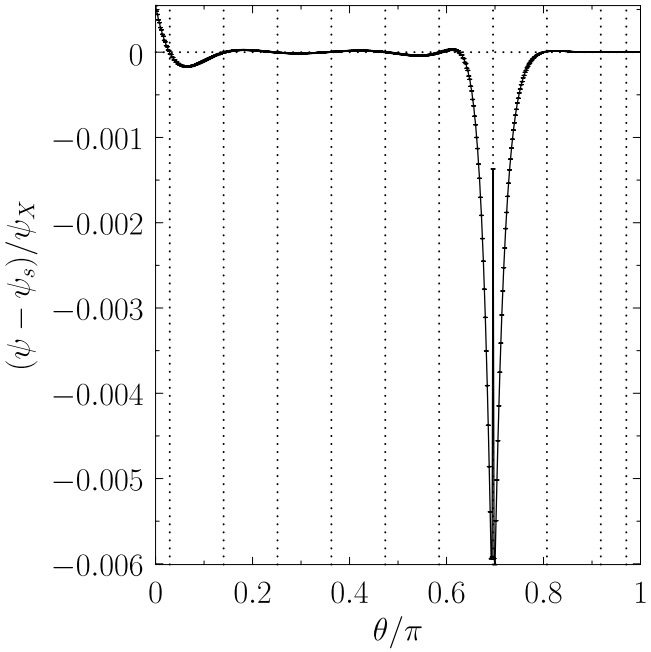

Figure 2. Difference between our solution, $\psi(r,z)$, and the Solov'ev solution, $\psi_s(r,z)$, on the LCFS, $\psi = \psi_X$, for a double-null magnetic equilibrium with $R = 1.0$, $a = 1.2$, $b = -1.0$, $c_0 = 1.1$, and $N_h = 10$. The vertical lines indicate the matching points. The X-points lie at $\theta/\pi = \pm 0.696$.

Let $\psi_s(r,z)$ denote the Solov'ev solution, (7), and let $\psi(r,z)$ represent our solution. We find that the value of $|\psi-\psi_s|/\psi_X$, averaged over the plasma volume, is 6.6×10^{-4}, whereas the maximum value is 5.6×10^{-3}. Figure 2 shows the difference between our solution and the Solov'ev solution on the LCFS. Of course, these two solutions should be identical on this flux-surface. It can be seen that the relative deviation between the two solutions peaks at the X-points, taking the value 6×10^{-3}.

Figures 3 and 4 show $\psi(r,z)/\psi_X$ profiles calculated by our method along horizontal and vertical lines in the r, z plane that pass through the magnetic axis. These profiles are compared to the equivalent Solov'ev profiles. It can be seen that our method accurately reconstructs the Solov'ev analytic solution within the plasma, but deviates strongly from this solution in the surrounding vacuum region. Moreover, both ψ and its spatial derivatives are clearly continuous across the LCFS.

To reiterate, inside the plasma, our solution for $\psi(r,z)$ coincides with a known analytic solution of the Grad–Shafranov

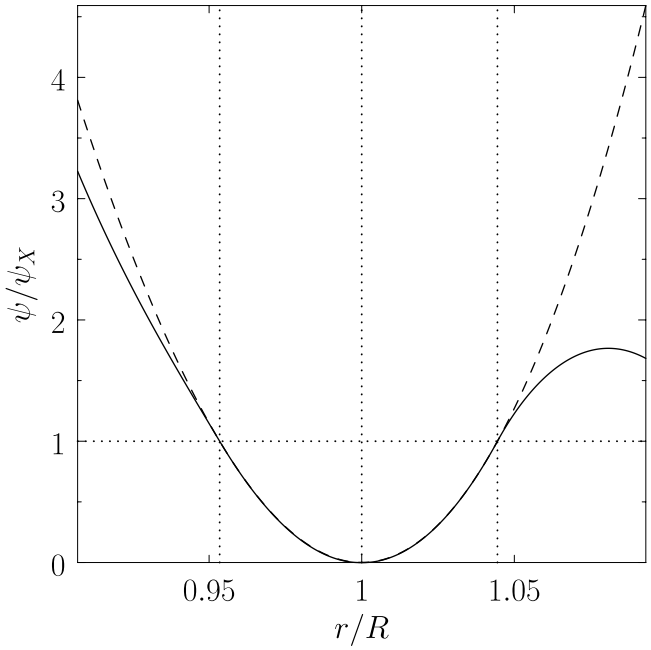

Figure 3. The solid curve shows $\psi(r,0)/\psi_X$ calculated by our method for a double-null magnetic equilibrium with $R = 1.0$, $a = 1.2$, $b = -1.0$, $c_0 = 1.1$, and $N_h = 10$. The dashed curve shows the corresponding Solov'ev solution. The horizontal and vertical dotted lines indicate the locations of the magnetic axis and the magnetic separatrix.

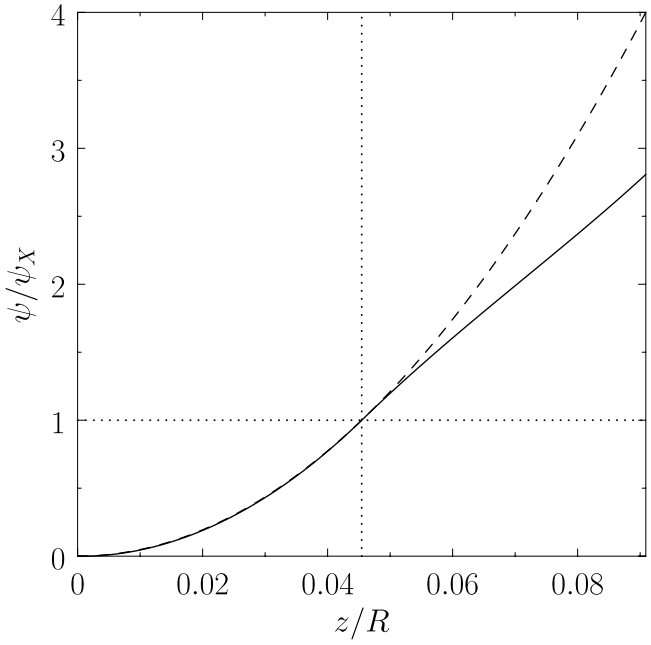

Figure 4. The solid curve shows $\psi(R,z)/\psi_X$ calculated by our method for a double-null magnetic equilibrium with $R = 1.0$, $a = 1.2$, $b = -1.0$, $c_0 = 1.1$, and $N_h = 10$. The dashed curve shows the corresponding Solov'ev solution. The horizontal and vertical dotted lines indicate the location of the magnetic separatrix.

equation. Moreover, outside the plasma, our solution is a homogeneous solution of the Grad–Shafranov equation that is generated by a combination of the known plasma currents and currents at infinity. Finally, our solution and its spatial derivatives are continuous across the LCFS. These facts conclusively demonstrate the validity of our method.

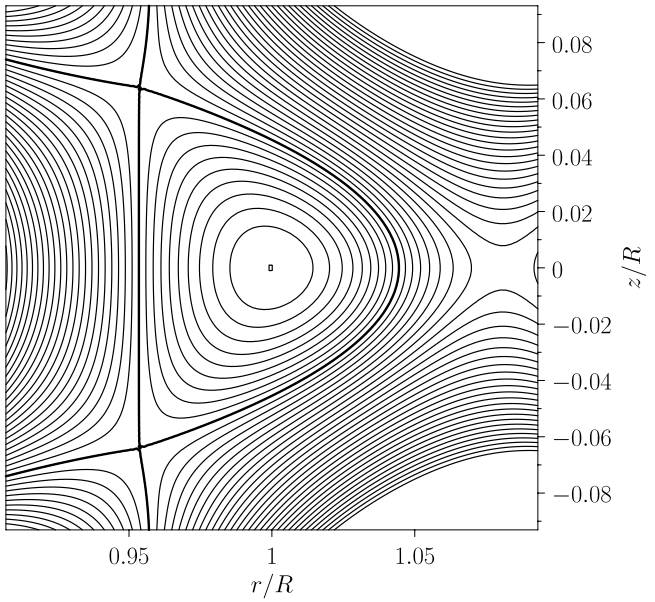

Figure 5. Contours of $\psi(r,z)$ calculated by our method for double-null magnetic equilibrium with $R = 1.0$, $a = 1.2$, $b = -1.0$, $c_0 = 1.1$, and $N_h = 10$. Note that the same contour levels are plotted as those that feature in figure 1.

Figure 5 shows contours of $\psi(r,z)$ calculated by our method for the case in hand. It can be seen, by comparison with figure 1, that the contours coincide with those of the Solov'ev solution inside the plasma, but are very different in the vacuum region surrounding the plasma. Note, in particular, the distorted magnetic X-points on the LCFS. There is a simple explanation for this phenomenon. In the Solov'ev solution, it is easily demonstrated that the two $\psi = \psi_X$ contours that cross at either the upper or the lower X-point subtend an acute angle

$$\Theta_p = \tan^{-1}\left[8\left(\frac{c_0}{-b}\right)\left(\frac{b+c_0}{a-c_0}\right)\right]^{1/2} \tag{36}$$

with one another. For the case in hand, $\Theta_p = 71.4°$. In our solution, we expect the $\psi = \psi_X$ contours bordering the plasma-filled quadrant of the X-point to subtend the same angle. On the other hand, in accordance with a well-known general principle, we expect the $\psi = \psi_X$ contours bordering the three vacuum-filled quadrants to cross at right angles. There is an obvious inconsistency here, which is due to the fact that there is a significant toroidal current density present in the plasma-filled quadrant, all the way to the magnetic separatrix, whereas there is zero current density in the vacuum-filled quadrants. The net result is that the vacuum-filled quadrant directly opposite the plasma-filled quadrant becomes distended.

5. Our method for single-null equilibria

Conventional tokamak equilibria are generally up–down-asymmetric, with a single magnetic null on the LCFS that lies below the magnetic axis. We can easily extend our analysis to take such equilibria into account by writing

$$\psi(r,z) = \frac{1}{2}\,(b+c_0)\,R^2\,z^2 + c_0\,R\,\zeta\,z^2 + c_1\,R^2\,\zeta\,z + \frac{1}{2}\,(a-c_0)\,R^2\,\zeta^2. \tag{37}$$

Note that the previous expression is an exact analytic solution of the Grad–Shafranov equation corresponding to the toroidal current distribution (6). The magnetic axis still lies at $r = R$, $z = 0$, $\psi = 0$. The magnetic X-points lie at $\zeta = \zeta_1$, $z = z_1$, $\psi = \psi_1$ and $\zeta = \zeta_2$, $z = z_2$, $\psi = \psi_2$. Here, z_1 and z_2 are the positive and negative roots, respectively, of the quadratic equation

$$2\,c_0^2\,z^2 + 3\,c_0\,c_1\,R\,z + [c_1^2 - (a-c_0)\,(b+c_0)]\,R^2 = 0. \tag{38}$$

Once z_1 and z_2 have been determined, ζ_1, ζ_2, ψ_1, and ψ_2 are obtained from

$$\zeta_{1,2} = -\frac{(b+c_0)\,R\,z_{1,2}}{2\,c_0\,z_{1,2} + c_1\,R}, \tag{39}$$

$$\psi_{1,2} = \frac{1}{2}\,(b+c_0)\,R^2\,z_{1,2}^2 + c_0\,R\,\zeta_{1,2}\,z_{1,2}^2 + c_1\,R^2\,\zeta_{1,2}\,z_{1,2} + \frac{1}{2}\,(a-c_0)\,R^2\,\zeta_{1,2}^2. \tag{40}$$

If $c_1 < 0$ then $0 < \psi_2 < \psi_1$. Hence, we can take $\psi = \psi_2$ as the LCFS. In this case, the LCFS only intersects a single magnetic X-point, which lies in the lower half plane ($z < 0$). From now on, we shall write $\psi_2 = \psi_X$, for the sake of consistency with our previous analysis.

Slightly generalizing our previous analysis, the poloidal magnetic flux generated by the toroidal plasma currents flowing within the plasma is

$$\psi_p(r,z) = -\int_0^{(1-\eta)\,\psi_X} \oint \frac{\sqrt{r\,r'}}{2\pi}\,\frac{[(2-k^2)\,K(k) - 2\,E(k)]}{k}\left(a + \frac{b\,R^2}{r'^2}\right) \times \left[\frac{\zeta'^2 + z'^2}{3\,c_0\,\zeta'\,z'^2 + 2\,c_1\,R\,\zeta'\,z' + (a-c_0)\,R\,\zeta'^2 + (b+c_0)\,R\,z'^2}\right] \times \mathrm{d}\psi\,\mathrm{d}\theta, \tag{41}$$

where

$$0 = (c_0\,R\,\tan^2\theta)\,\zeta'^3 + \left[c_1\,R^2\,\tan\theta + \frac{1}{2}\,(b+c_0)\,\tan^2\theta\,R^2 + (a-c_0)\,R^2\right]\zeta'^2 - \psi, \tag{42}$$

$$r' = \sqrt{2\,R\,\zeta' + R^2}, \tag{43}$$

$$z' = \tan\theta\;\zeta'. \tag{44}$$

The poloidal magnetic flux generated by currents flowing in distant magnetic field coils takes the form [13]

$$\psi_h(r,z) = \sum_{N=0,N_h}^{N\neq 1} c_N\,\psi_N(r,z), \tag{45}$$

where the c_N are arbitrary coefficients. When N is even,

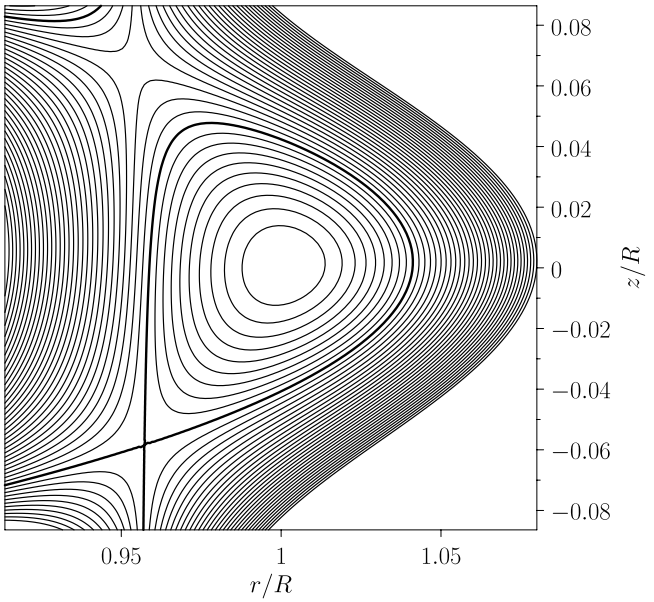

Figure 6. Contours of $\psi(r,z)$ calculated by Solov'ev's method for a single-null magnetic equilibrium with $R = 1.0$, $a = 1.2$, $b = -1.0$, $c_0 = 1.1$, and $c_1 = -0.005$.

$$\psi_N(r,z) = \sum_{n=0,N/2-1} A_N^n\,r^{N-2\,n}\,z^{2\,n}, \tag{46}$$

and

$$A_N^n = -\frac{(N/2+1-n)\,(N/2-n)}{n\,(n-1/2)}\,A_N^{n-1} \tag{47}$$

for $1 \leqslant n \leqslant N/2-1$, with $A_N^0 = 1$. On the other hand, when N is odd,

$$\psi_N(r,z) = \sum_{n=0,(N-3)/2} A_N^n\,r^{N-2\,n-1}\,z^{2\,n+1}, \tag{48}$$

and

$$A_N^n = -\frac{(N/2+1/2-n)\,(N/2-1/2-n)}{n\,(n+1/2)}\,A_N^{n-1} \tag{49}$$

for $1 \leqslant n \leqslant (N-3)/2$, with $A_N^0 = 1$. Note that the sum (45) is truncated at $N = N_h$. Incidentally, $N = 1$ is excluded from the sum because $\psi_1 = 0$. The sum (45) differs from the sum (32) because it incorporates up–down-asymmetric (i.e. odd N) homogeneous solutions of the Grad–Shafranov equation. These solutions were previously excluded because double-null equilibria are up–down symmetric.

The coefficients, c_N, that characterize the homogenous solution, (45), are determined by demanding that

$$\psi_p(r,z) + \psi_h(r,z) = (1-\eta)\,\psi_X \tag{50}$$

on the control surface $\psi = (1-\eta)\,\psi_X$. Given that there are N_h independent c_N values, the matching must be performed at N_h different values of θ. These values are evenly distributed in the range 0 to 2π, with a small common offset that is chosen so as to ensure that one of the matching points corresponds to the magnetic X-point on the LCFS.

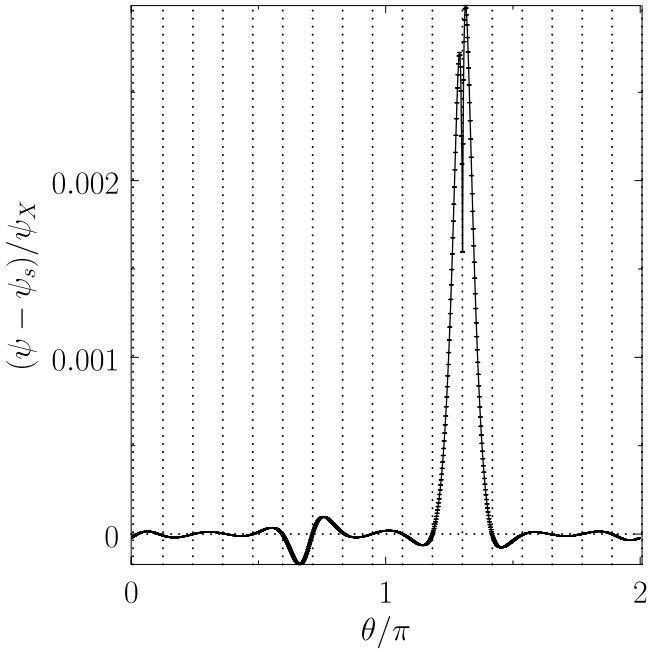

Figure 7. Difference between our solution, $\psi(r,z)$, and the Solov'ev solution, $\psi_s(r,z)$, on the LCFS, $\psi=\psi_X$, for a single-null magnetic equilibrium with $R=1.0$, $a=1.2$, $b=-1.0$, $c_0=1.1$, $c_1=-0.005$, and $N_h=18$. The vertical lines indicate the matching points. The X-point lies at $\theta/\pi=1.30$.

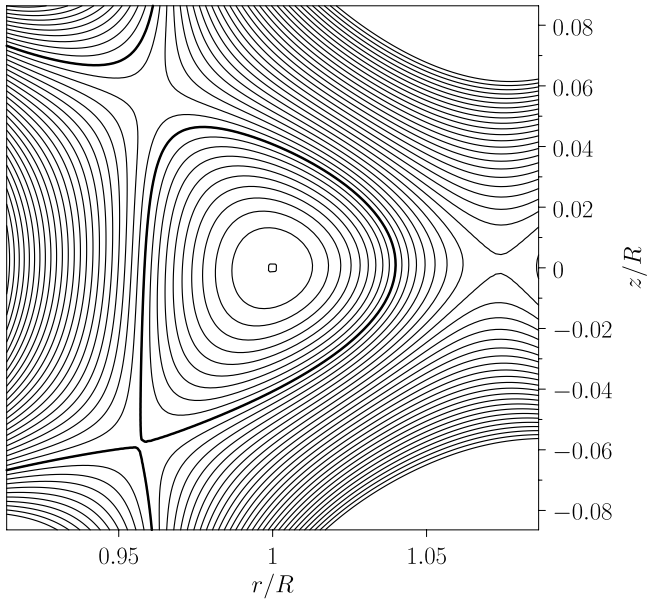

Figure 8. Contours of $\psi(r,z)$ calculated by our method for a single-null magnetic equilibrium with $R=1.0$, $a=1.2$, $b=-1.0$, $c_0=1.1$, $c_1=-0.005$, and $N_h=18$. Note that the same contour levels are plotted as those that feature in figure 6.

Our second example is an up–down-asymmetric single-null plasma equilibrium calculated with the following parameters: $R=1.0$, $a=1.2$, $b=-1.0$, $c_0=1.1$, and $c_1=-0.005$. The corresponding Solov'ev solution is shown in figure 6.

As before, the $\psi-\theta$ integral in expression (41) is implemented using a 2D trapezium rule on a 1000×1000 uniform rectangular grid. The regularization parameters ϵ and η again take the values 10^{-12} and 10^{-6}, respectively. We find that the previously defined error parameter, λ, attains its minimum value, 9×10^{-4}, when $N_h=18$.

We find that the value of $|\psi-\psi_s|/\psi_X$, averaged over the plasma volume, is 3.4×10^{-3}, whereas the maximum value is 7.7×10^{-3}. Figure 7 shows the difference between our solution and the Solov'ev solution on the LCFS. Of course, these two solutions should be identical on this flux-surface. It can be seen that the relative deviation between the two solutions peaks at the X-point, taking the value 3×10^{-3}.

Figure 8 shows contours of $\psi(r,z)$ calculated by our method for the case in hand. It can be seen, by comparison with figure 6, that the contours coincide with those of the Solov'ev solution inside the plasma, but are very different in the vacuum region surrounding the plasma. As before, the magnetic X-point on the LCFS is distorted in such a manner that the vacuum-filled quadrant directly opposite the plasma-filled quadrant becomes distended. The explanation for this phenomenon is the same as that given in the previous section.

6. Summary

In this paper, we calculate a tokamak equilibrium generated by a combination of currents flowing within the plasma and in distant external magnetic field coils. The poloidal magnetic flux surfaces inside the plasma are identical to those given by the well-known exact analytic solution of the Grad–Shafranov equation due to Solov'ev. However, the flux surfaces outside the plasma correspond to a properly matched vacuum solution. We use a Green's function method to compute the poloidal magnetic flux generated by the known plasma currents, together with a parameterized homogeneous solution to the Grad–Shafranov equation (that is well-behaved at small r and z), to construct the vacuum solution. The vacuum solution is matched to the analytic solution on the last closed magnetic flux surface (LCFS) to determine the parameters in the homogeneous solution. This procedure is performed for both up–down-symmetric double-null and up–down-asymmetric single-null equilibria. We find that any magnetic X-points on the LCFS are distorted due to the fact that one quadrant is filled by a current-carrying plasma, whereas the other three are filled by a vacuum in which no current flows. In particular, the vacuum quadrant directly opposite the plasma-filled quadrant expands at the expense of the other three quadrants. We conjecture that this phenomenon could be a feature of any magnetically diverted tokamak equilibrium in which there is a large toroidal current density at edge of the plasma (as is indeed generally the case in H-mode equilibria). Finally, the method described in this paper could easily be modified to deal with the extended Solov'ev-type equilibria described in [9–11].

Acknowledgments

The authors thank L. Zheng and M.T. Kotschenreuther (IFS, University of Texas at Austin) for proposing the research contained in this paper, and for alerting them to the fact that the plasma-filled quadrant of a magnetic diverter does not

necessarily subtend 90 degrees if the plasma current on the LCFS is non-zero, which is inconsistent with the standard scenario in which the field-lines that cross at a magnetic X-point are assumed to do so at right-angles. The authors also thank F.L. Waelbroeck (IFS, University of Texas at Austin) for helpful discussions. This work was funded by the US Department of Energy under Contract DE-FG02-04ER-54742. T.X. was funded by the China Scholarship Council and the ITER Special Foundation of China under Contract 2017YFE0301202.

References

[1] Grad H. and Rubin H. 1958 Hydromagnetic equilibria and force-free fields *Proc. of 2nd UN Conf. on Peaceful Uses of Atomic Energy (Geneva, Switzerland, 1–13 September 1958)* vol 31, p 190 (https://inis.iaea.org/search/search.aspx?orig_q=RN:39082408)

[2] Shafranov V.D. 1958 On magetohydrodynamical equilibrium configurations *Sov. Phys.—JETP* **6** 545

[3] Lüst R. and Schlüter A. 1957 Axialsymmetrische magnetohydrodynamische gleichgewichtskonfigurationen *Z. Naturforsch.* A **12a** 850

[4] Solov'ev L.S. 1968 The theory of hydromagnetic stability of toroidal plasma configurations *Sov. Phys.—JETP* **26** 400

[5] Johnson J.L. *et al* 1979 Numerical determination of axisymmetric toroidal magnetohydrodynamic equilibria *J. Comput. Phys.* **32** 212

[6] Lao L.L., Hirshman S.P. and Weiland R.M. 1981 Variational moment solutions to the Grad–Shafranov equation *Phys. Fluids* **24** 1431

[7] Green B.J. and Zehrfeld H.P. 1977 Local, ideal and resistive stability in tokamaks with non-circular cross-section *Nucl. Fusion* **17** 1133

[8] Weening R.H. 2000 Analytic spherical torus plasma equilibrium model *Phys. Plasmas* **7** 3654

[9] Guazzotto L. and Freidberg J.P. 2007 A family of analytic equilibrium solutions for the Grad–Shafranov equation *Phys. Plasmas* **14** 112508

[10] Shi B. 2009 Exact single-null diverted tokamak equilibria *Plasma Phys. Control. Fusion* **51** 105008

[11] Cerfon A.J. and Freidberg J.P. 2010 'One size fits all' analytic solutions to the Grad–Shafranov equation *Phys. Plasmas* **17** 032502

[12] Jackson J.D. 1999 *Classical Electrodynamics* 3rd edn (New York: Wiley) p 182

[13] Reusch M.F. and Neilson G.H. 1986 Toroidally symmetric polynomial multipole solutions of the vector Laplace equation *J. Comput. Phys.* **64** 416